## Magnetic Penetration Depth Measurements of $Pr_{2-x}Ce_xCuO_{4-\delta}$ Films on Buffered Substrates: Evidence for a Nodeless Gap

Mun-Seog Kim, John A. Skinta, and Thomas R. Lemberger Department of Physics, Ohio State University, Columbus, OH 43210-1106

A. Tsukada and M. Naito

NTT Basic Research Laboratories, 3-1 Morinosato Wakamiya, Atsugi-shi, Kanagawa 243, Japan

We report measurements of the inverse squared magnetic penetration depth,  $\lambda^{-2}(T)$ , in  $\Pr_{2-x}\operatorname{Ce}_x\operatorname{CuO}_{4-\delta}$  (0.115  $\leq x \leq 0.152$ ) superconducting films grown on  $\operatorname{SrTiO}_3$  (001) substrates coated with a buffer layer of insulating  $\Pr_2\operatorname{CuO}_4$ .  $\lambda^{-2}(0)$ ,  $T_c$  and normal-state resistivities of these films indicate that they are clean and homogeneous. Over a wide range of Ce doping,  $0.124 \leq x \leq 0.144$ ,  $\lambda^{-2}(T)$  at low T is flat: it changes by less than 0.15% over a factor of 3 change in T, indicating a gap in the superconducting density of states. Fits to the first 5% decrease in  $\lambda^{-2}(T)$  produce values of the minimum superconducting gap in the range of  $0.29 \leq \Delta_{\min}/k_B T_c \leq 1.01$ .

It is still a puzzle whether pairing symmetry in n-type cuprates is d wave or not[1, 2, 3, 4, 5, 6, 7, 8, 9]. Recently, novel concepts on pairing symmetry of n- and p-type cuprates have come forward: a possible transition in pairing symmetry [10, 11] and/or a mixed symmetry order parameter[12, 13, 14]. Our previous work[10] involved  $La_{2-x}Ce_xCuO_{4-\delta}$  (LCCO) and  $Pr_{2-x}Ce_xCuO_{4-\delta}$ (PCCO) films grown directly on SrTiO<sub>3</sub> substrates. We found that at low Ce doping levels,  $\lambda^{-2}(T)$  at low T was quadratic in T, but at higher dopings,  $\lambda^{-2}(T)$  showed activated behavior. These results suggested a d- to s-wave pairing transition near optimal doping, as was also suggested by tunneling experiments[11] on PCCO films. We have subsequently improved film quality by eliminating the interface between the film and substrate, by growing PCCO films onto Pr<sub>2</sub>CuO<sub>4</sub> (PCO)/SrTiO<sub>3</sub> instead of directly onto SrTiO<sub>3</sub>. The insulating PCO layer is thought to lessen lattice mismatch between PCCO film and SrTiO<sub>3</sub> substrate, so that these films should be more homogeneous through their thickness. In fact, their normal state resistivities are somewhat lower than those of unbuffered PCCO films for the same doping, x.  $T_c$ 's at optimal doping in the two film families are the same,  $T_c \simeq 24 \text{ K}.$ 

Films were prepared by molecular-beam epitaxy (MBE) on  $10~\rm mm \times 10~\rm mm \times 0.35~\rm mm~SrTiO_3$  substrates as detailed elsewhere[15]. The same growth procedures and parameters were used for all films. For all films, PCCO and PCO layers are 750 Å and 250 Å thick, respectively. Ce concentrations, x, are measured to better than  $\pm 0.005$  by inductively coupled plasma spectroscopy. X-ray rocking curves show full-width at half maximum of (006) reflection for all films to be less than  $0.4^{\circ}$ , which implies that the films are highly c-axis oriented.

The penetration depth,  $\lambda(T)$ , was measured down to  $T \simeq 0.5$  K using a mutual inductance apparatus, described in detail elsewhere [16, 17], in a He<sup>3</sup> refrigerator. The system temperature was measured with a Cernox resistor (LakeShore Inc.) and its reliability, below 1 K, was

confirmed by measuring the superconducting transition temperature of a Zn plate,  $T_c = 0.875$  K.

Each film was centered between drive and pick-up coils with diameters of  $\sim 1$  mm. A small current at 50 kHz in the drive coil induced diamagnetic screening currents in the film, i.e., parallel to the CuO<sub>2</sub> planes. The time derivative of the net magnetic field from drive coil and induced current in the film was measured as a voltage across the pick-up coil. The real and imaginary parts of the mutual inductance are proportional to the quadrature and in-phase components of ac voltage, respectively. Because the coils were much smaller than the film, the applied field was concentrated near the center of the films, and demagnetizing effects at the film perimeter were not relevant. Because films were thinner than  $\lambda$ , the current density induced in the films was essentially uniform through the film thickness. Nonlinear effects occur only very close to  $T_c$  where  $\lambda^{-2}$  is less than 1% of its value at T=0. All data presented here represent linear response.

The procedure to extract  $\lambda^{-2}(T)$  from the measured mutual inductance is the following. First, a constant background mutual inductance due to stray couplings between drive and pickup circuits is subtracted from raw data. This background is the measured mutual inductance at 4.2 K with the sample replaced by a 100 micronthick superconducting Pb foil with identical shape and area. No magnetic field passes through the Pb foil. A glass shim ensures that the spacing between coils is the same as with the real sample. The adjusted data are normalized to the mutual inductance measured above  $T_c$ , at  $T \sim 30$  K, where the film is utterly transparent to the ac field. Normalization reduces uncertainties associated with amplifier gains and nonideal aspects of the coil windings. A numerical model of the drive and pick-up coils enables us to convert the subtracted and normalized mutual inductance to sheet conductivity:  $\sigma d = \sigma_1 d - i\sigma_2 d$ , where d is film thickness. Finally,  $\lambda^{-2}$  is determined from  $\sigma_2 d$  via:  $\sigma_2 = 1/\mu_0 \omega \lambda^2$ , where  $\mu_0$  is the magnetic permeability of vacuum and  $\omega$  is the angular frequency of the

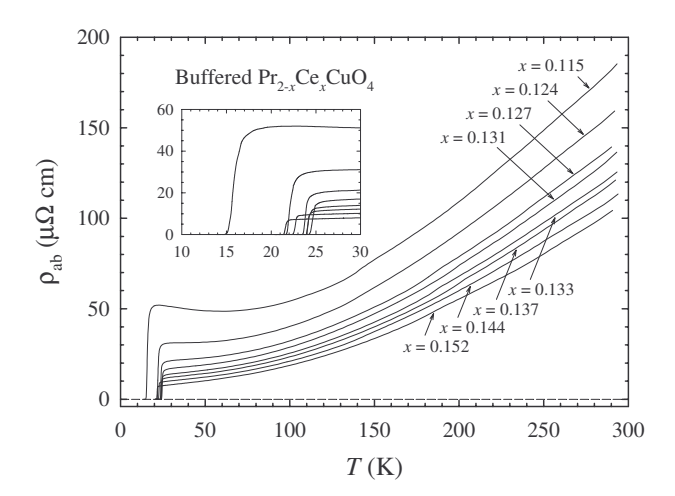


FIG. 1: ab-plane resistivities,  $\rho_{ab}(T)$ , of buffered  $\Pr_{2-x}\operatorname{Ce}_x\operatorname{CuO}_{4-\delta}$  films. For resistivities at T=25 K, see Table I. Inset:  $\rho_{ab}(T)$  around  $T_c$ .

drive current. The absolute accuracy of  $\lambda^{-2}$  is limited by  $\pm 10\%$  uncertainty in d. The T dependence of  $\lambda^{-2}$  is unaffected by this uncertainty.

Except for differences in the flatness of  $\lambda^{-2}$  at low T, which is the focal point of this paper, buffered films are very much like unbuffered films reported earlier[10]. Fig. 1 shows in-plane resistivity,  $\rho_{ab}(T)$ , for buffered PCCO films.  $\rho_{ab}$  in the normal state decreases smoothly and monotonically with Ce doping, x, even for small changes in x, implying that the main difference among films is Ce content. If there were random variations in degree of epitaxy, structural defects, etc., then resistivity would not be such a smooth function of x. These resistivities are slightly smaller than for PCCO films without buffer layers[9, 10], and significantly lower than for NCCO and PCCO crystals[3, 18]. The inset of Fig. 1 shows that resistive transitions are reasonably sharp, and that  $T_c$  is a weak function of Ce concentration, although resistivity is not. Table I summarizes properties of the films.

Fluctuations cause  $\sigma_1(T)$  to peak at the superconducting transition. Hence,  $\sigma_1(T)$  is a much more stringent test of film quality than resistivity. For example, if  $T_c$  varies through the film thickness, resistivity reveals only the highest  $T_c$ . Because our probing magnetic field passes through the film,  $\sigma_1(T)$  has a peak at the  $T_c$  of every layer. Transitions associated with small bad spots in the film, as opposed to an entire film layer, are distinguished by their having essentially no effect on the superfluid response,  $\sigma_2$ . When a layer goes superconducting there is a distinct change in the slope of  $\lambda^{-2}(T)$ .

 $\sigma_1(T)$ 's of buffered PCCO films (Fig. 2) show that several of them have a double transition, reflected as shoulder (x = 0.115, 0.124, and 0.137) or satellite (x = 0.144 and 0,152) structure of peaks. We define two transition temperatures,  $T_{c1}$  and  $T_{c2}$ , from peaks in  $\sigma_1(T)$ , where  $T_{c1} > T_{c2}$ . The resistive  $T_c$  is always at the onset of the

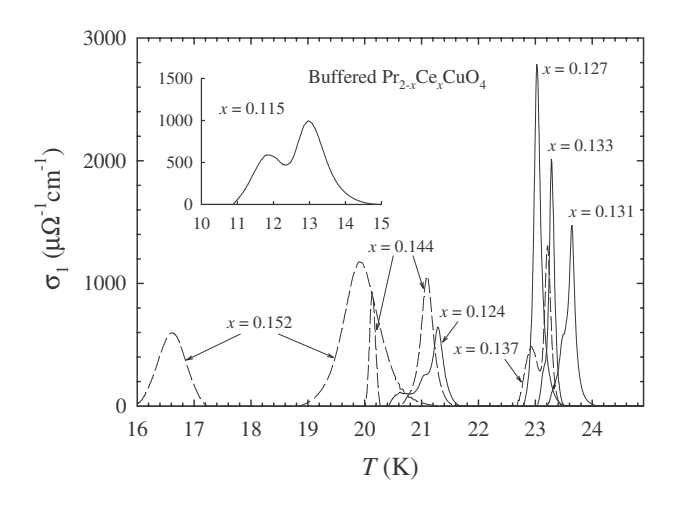


FIG. 2:  $\sigma_1(T)$  at 50 kHz in buffered  $\Pr_{2-x}\text{Ce}_x\text{CuO}_{4-\delta}$  films. Inset:  $\sigma_1(T)$  for the film with x=0.115.

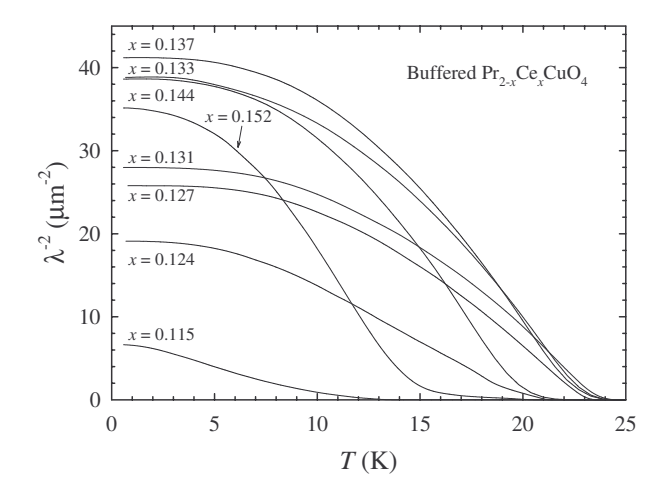


FIG. 3:  $\lambda^{-2}(T)$  for buffered  $\Pr_{2-x} \operatorname{Ce}_x \operatorname{CuO}_{4-\delta}$  films. Filmto-film uncertainty in  $\lambda^{-2}(0)$  is  $\sim \pm 10\%$ .

 $T_{c1}$ -peak. For the films most important to the conclusions of this paper,  $0.124 \le x \le 0.144$ , the width of the  $T_{c1}$  peak,  $\Delta T_{c1}$ , is  $\le 1$  K, indicating excellent film homogeneity. The peak at  $T_{c2}$  most likely involves a bad spot in the film, since there is no corresponding feature in the slope of  $\lambda^{-2}(T)$ , (see Fig. 3). Accordingly, the lower transition is neglected in our analysis. Films with highest and lowest Ce concentrations (x = 0.115 and 0.152) have broader transition widths ( $\Delta T_c = 2.4 \sim 3.9$  K) than other films, perhaps because  $T_c$  is more sensitive to x.

Figure 3 shows  $\lambda^{-2}(T)$  for all films.  $\lambda^{-2}(0)$  vs. x increases rapidly for  $x \leq 0.133$ , and it is constant or decreases slowly for x > 0.133. Values of  $\lambda^{-2}(0)$  are slightly higher than for unbuffered films. The surprising upward curvature that develops in  $\lambda^{-2}(T)$  near  $T_c$  at high Ce concentrations was also observed in unbuffered LCCO and PCCO films[9, 10].

In our previous work[10] on unbuffered PCCO films,

films with low Ce concentrations showed quadratic  $(T^2)$  behavior in  $\lambda^{-2}(T)$  at low T. Films with high Ce concentrations showed gap-like behavior:

$$\lambda^{-2}(T) \simeq \lambda^{-2}(0)[1 - C_{\infty} \exp(-D/t)],$$
 (1)

where  $C_{\infty}$  and D are adjustable parameters, and  $t = T/T_c$ . In the clean limit, D is approximately the minimum gap on the Fermi surface, normalized to  $k_BT_c$ , and  $C_{\infty}$  is roughly twice the average superconducting density of states (DOS) over energies within  $k_BT$  of the gap edge. For isotropic BCS superconductors, the best-fit value of  $C_{\infty}/2$  is about 2.2. The change in low-T behavior of  $\lambda^{-2}(T)$  near optimal doping suggested a transition in pairing symmetry.

We now turn to the low-T behavior of  $\lambda^{-2}(T)$  for buffered PCCO films, shown on a greatly expanded scale in Fig. 4. The most important thing to notice is that  $\lambda^{-2}(T)$  is flat to better than 0.15% over a factor of 3 or more change in T. Residual variations in  $\lambda^{-2}(T)$  at the 0.1% level are due, at least in part, to slow drift in the gain of the lock-in amplifiers used to measure current and voltage. These data are incompatible with simple dwave models with nodes in the gap. Thus, except for the most underdoped and overdoped films (x = 0.115 and 0.152),  $\lambda^{-2}(T)$  shows gapped behavior. Recent angleresolved photoemission spectroscopy measurements [2] indicate well-defined quasiparticle states on the Fermi surface where the  $d_{x^2-y^2}$  node would be, so the gapped behavior that we observed could not be ascribed to a Fermi surface effect.

To estimate the gap, we fit Eq. (1) to the first  $\sim 5\%$ drop in  $\lambda^{-2}(T)$ , (thin solid lines in Fig. 4). It comes as no surprise that quadratic fits over the same temperature range are unacceptable (dashed lines). For films with x =0.115 and 0.152, data at T < 0.5 K are needed to distinguish between  $T^2$  and  $e^{-D/t}$ . Values of the minimum gap,  $\Delta_{\min} = Dk_BT_c$  and average DOS,  $C_{\infty}/2$ , extracted from the above exponential fits are presented in Table I. D values are significantly lower than the BCS weak-couplinglimit value, 1.76, for s-wave superconductors (2.14 for d-wave superconductors). D is largest,  $D \sim 1$ , for x near 0.13. A similar value,  $D \simeq 0.85$ , was found for unbuffered PCCO films [9] with the same Ce concentration. Values of  $C_{\infty}/2$  ( $\ll$  1) are also much smaller than for weakcoupling isotropic s wave. This implies existence of a peak in the DOS for a certain  $E \ (> \Delta_{\min})$ , because the states should be conserved.

The next question is: where is the peak in the DOS, i.e., how big is the maximum gap,  $\Delta_{\text{max}}$ , on the Fermi surface? To answer this question, we employ a model anisotropic gap function and the clean-limit result that  $1 - \lambda^{-2}(T)/\lambda^{-2}(0)$  is an integral of quasiparticle DOS times the derivative of the Fermi function with respect to energy[19]. Fig. 5 shows a good fit to  $\lambda^{-2}(T)$  for film with x = 0.131 using the DOS in the inset. In this fit, the minimum gap was fixed at the value found by fitting

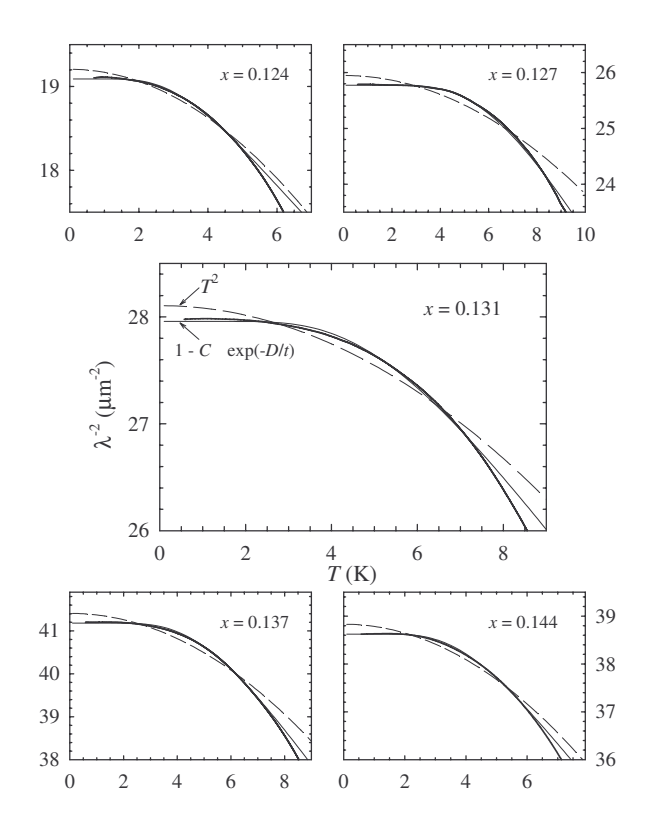


FIG. 4: Expanded view of  $\lambda^{-2}(T)$  at low T for buffered  $\Pr_{2-x}\operatorname{Ce}_x\operatorname{CuO}_{4-\delta}$  films. Thin solid and dashed lines denote best fits of  $\lambda^{-2}(0)[1-C_\infty\exp(-D/t)]$  and  $\lambda^{-2}(0)[1-(T/T_0)^2]$  to the first 5% drop in  $\lambda^{-2}(T)$ , respectively.

the low-T data, i.e.,  $\Delta_{\rm min}/k_BT_c=0.99$ . Then, as one can see in inset of Fig. 5, the average DOS within  $\sim k_BT$  of the minimum gap edge agrees well with  $C_{\infty}/2=0.5$  from Table I. For film with x=0.131,  $\Delta_{\rm max}$  is about  $2.6k_BT_c$  ( $\pm15\%$ ).

We emphasize that we cannot say anything about the shape of the peak in the DOS, only its location. An equally acceptable fit, with a similar peak energy, is obtained even when the sharp narrow peak in the inset of Fig. 5 is replaced by a rectangular peak[20].

In summary, we measured the inverse squared magnetic penetration depth,  $\lambda^{-2}(T)$ , of several  $\Pr_{2-x}\mathrm{Ce}_x\mathrm{CuO}_{4-\delta}$  films on buffered  $\Pr_2\mathrm{CuO}_4/\mathrm{SrTiO}_3$  substrates down to  $T/T_c < 0.03$ . Overall, the resistivities and penetration depths were similar to films grown directly on  $\Pr_3$ . However, for PCCO films on buffered substrates,  $\lambda^{-2}(T)$  at low T exhibits gapped behavior over a wide range of Ce doping, including underdoping. This implies a superconducting gap without nodes on the Fermi surface. Values of the minimum superconducting gap for the films are in range of  $0.3 \le \Delta_{\min}/k_BT_c \le 1.0$ . We cannot distinguish among models with various gap symmetries, e.g., anisotropic s, s+id, or d+id.

The research at OSU was supported by NSF Grant No. DMR-0203739.

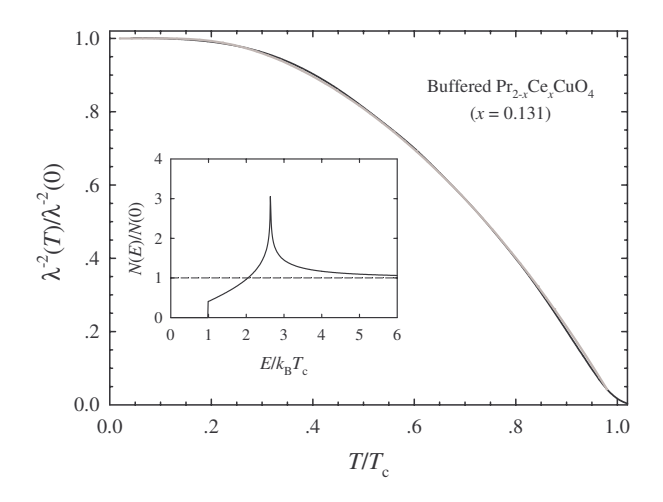


FIG. 5:  $\lambda^{-2}(T)$  for  $\Pr_{1.869}\text{Ce}_{0.131}\text{CuO}_{4-\delta}$  film. Gray line shows an excellent fit obtained with density of states shown in the inset. Inset: Quasiparticle density of states in  $s+id_{x^2-y^2}$  gap symmetry.

TABLE I: Properties of eight MBE-grown  $\Pr_{2-x}\operatorname{Ce}_x\operatorname{CuO}_{4-\delta}$  films on  $\Pr_2\operatorname{CuO}_4/\operatorname{SrTiO}_3$ .  $T_c$  (or  $T_{c1}$ ) and  $T_{c2}$  are locations of main and secondary peaks in  $\sigma_1(T)$ , respectively.  $\Delta T_c$  is full width of the (main) peak in  $\sigma_1(T)$ .  $\rho_{ab}(25\text{ K})$  is the ab-plane resistivity at T=25 K.  $\lambda^{-2}(0)$ ,  $C_{\infty}/2$ , and  $D=\Delta_{\min}/k_BT_c$  are fit parameters, in Eq. (1).

$\overline{x}$	$T_c$ $(T_{c1})$	$T_{c2}$	$\Delta T_c$	$\rho_{ab}(25 \text{ K})$	$\lambda^{-2}(0)$	$C_{\infty}/2$	D
	(K)	(K)	(K)	$(\mu\Omega \mathrm{cm})$	$(\mu \mathrm{m}^{-2})$		
0.115	13.0	11.8	3.9	51.0	6.6	(0.21)	(0.29)
0.124	21.3	20.7	1.3	30.1	19.1	0.28	0.56
0.127	23.1		0.8	19.4	25.8	0.60	1.01
0.131	23.6		0.8	15.3	27.9	0.50	0.99
0.133	23.3		0.5	12.8	38.9	0.42	0.73
0.137	23.2	22.9	0.7	10.8	41.2	0.38	0.83
0.144	21.2	20.2	0.9	9.5	38.6	0.30	0.72
0.152	19.8	16.6	2.4	7.7	35.1	(0.17)	(0.37)

- C. C. Tsuei and J. R. Kirtley, Phys. Rev. Lett. 85, 182 (2000).
- [2] N. P. Armitage et al., Phys. Rev. Lett. 86, 1126 (2001).
- [3] J. D. Kokales *et al.*, Phys. Rev. Lett. **85**, 3696 (2000).
- [4] R. Prozorov, R. W. Giannetta, P. Fournier, and R. L. Greene, Phys. Rev. Lett. 85, 3700 (2000).
- [5] L. Alff et al., Phys. Rev. B 58, 11197 (1998).
- [6] S. Kashiwaya et al., Phys. Rev. B 57, 8680 (1998).
- [7] C.-T. Chen et al., Phys. Rev. Lett. 88, 227002 (2002).
- [8] L. Alff et al., Phys. Rev. Lett. 83, 2644 (1999).
- [9] J. A. Skinta, T. R. Lemberger, T. Greibe, and M. Naito, Phys. Rev. Lett. 88, 207003 (2002).
- [10] J. A. Skinta et al., Phys. Rev. Lett. 88, 207005 (2002).
- [11] A. Biswas et al., Phys. Rev. Lett. 88, 207004 (2002).
- [12] A. Kohen and G. Deutscher, cond-mat/0207382 (2002).
- [13] K. A. Müller, Phil. Mag. Lett. 82, 279 (2002).
- [14] D. Daghero, R. S. Gonnelli, G. A. Ummarino, and V. A. Stepanov, cond-mat/0207411 (2002).
- [15] M. Naito, H. Sato, and H. Yamamoto, Physica C 293, 36 (1997).
- [16] S. J. Turneaure, E. R. Ulm, and T. R. Lemberger, J. Appl. Phys. 79, 4221 (1996).
- [17] S. J. Turneaure, A. A. Pesetski, and T. R. Lemberger, J. Appl. Phys. 83, 4334 (1998).
- [18] J. D. Kokales et al., Physica C **341-348**, 1655 (2001).
- [19] M. Tinkham, Introduction to Superconductivity, 2nd ed. (McGraw-Hill, New York, 1996).
- [20] J. A. Skinta et al., cond-mat/0301174 (2003).